Derivation and analysis of an ordinary differential equation mean-field model for studying clinically recorded epilepsy dynamics

Frank Marten,[1] Serafim Rodrigues,[1] Piotr Suffczynski,[2] Mark P. Richardson,[3] and John R. Terry[1],*

[1]*Department of Engineering Mathematics, University of Bristol, Bristol, BS8 1TR, United Kingdom*[†]
[2]*Department of Biomedical Physics, Warsaw University, Poland*
[3]*Institute of Psychiatry, King's College London, Camberwell, SE5 8AF, United Kingdom*

In this paper we describe how an ordinary differential equation model of corticothalamic interactions may be obtained from a more general system of delay differential equations. We demonstrate that transitions to epileptic dynamics via changes in system parameters are qualitatively the same as in the original model with delay, as well as demonstrating that the onset of epileptic activity may arise due to regions of bistability. Hence, the model presents in one unique framework, two competing theories for the genesis of epileptiform activity. Similarities between model transitions and clinical data are presented and we argue that statistics obtained from, and a parameter estimation of this model may be a potential means of classifying and predicting the onset and offset of seizure activity.

PACS number(s): 87.19.−j, 05.45.−a, 87.18.−h

I. INTRODUCTION

Electroencephalography (EEG) is a technique for recording the brain's electrical activity [1]. The generators of this activity are primarily cortical nerve cell potentials. Specifically, cortical pyramidal cells receive both excitatory and inhibitory postsynaptic potentials, which in turn generate extracellular currents that effectively sum up into a macroscopic signal. This summation process is made possible due to the alignment of the apical dendrites of pyramidal cells perpendicular to the surface of the scalp, whereas the postsynaptic activity in dendrites of other neurons that are tangential to the scalp are not measured.

Close correlates between the dynamical activity patterns observed in EEG and the cognitive state of the subject have been inferred, and consequently EEG is frequently used as a diagnostic tool in subjects with a variety of neurological disorders [1]. In the past few years, there has been increasing interest in the use of mathematical models of macroscopic brain activity to explain transitions between different dynamical states observed in EEG [2–5], with a particular focus on understanding the transition between healthy and seizure states in epilepsy [4–9]. These recent works have focussed on a mean-field description of cortico-thalamic interactions, which have been implicated in detailed physiological studies [10] as being crucial in determining dynamical activity arising during sleep and epilepsy [11,20].

The focus of our research is a class of primary generalized seizures, absence seizures, which typically affect children and young adults. There is a classical waveform associated with such seizures, namely, a 3 Hz "spike and wave" (SW) discharge, that appears approximately synchronously across all EEG channels. However, closer inspection of such discharges reveals a much greater array of dynamical behavior, such as polyspike and wave, and wave-spike discharges. Examples of these rhythms are shown in Fig. 1. In addition, there are graded seizure onsets; in some seizures the spike evolves over a number of initial cycles of the seizure [as presented in Figs. 1(a) and 1(c)], whereas in others the spike appears immediately at the start of the seizure [for example, Figs. 1(b) and 1(d)]. These suggest that a number of different mechanisms may play a role in determining seizure dynam-
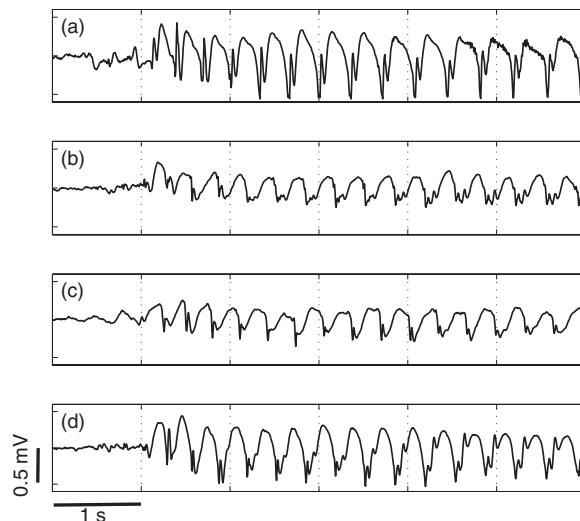

FIG. 1. Representative examples of four different absence seizures taken from a database covering 50 seizures from 20 subjects. In panel (a) we present a "classical" single spike and wave discharge of the sort often used to highlight absence epilepsy in the literature. In panels (b), (d) we observe that seizure can evolve dynamically, with for example the addition of an extra spike per cycle. Panels (c) and (d) illustrate that seizures may have different types of onset. For example, in panel (c) the seizure evolves gradually, with spikes appearing after an initial oscillation, whereas in panel (d) spikes appear abruptly at the start of high amplitude activity.

---

*J.R.Terry@bristol.ac.uk

[†]The study was approved by the local research ethics committee of King's College Hospital. This approval included the sharing of anonymized data with nonclinical collaborators.

ics and it is our desire to develop a unifying model that can capture the wide variety of such transitions.

II. MODEL DEVELOPMENT

In the present paper we discuss a neural mass model, which is based on our work in Ref. [12]. In this work, we used a delay differential equation (DDE) to simulate dynamics observed in patients with absence seizures. In the present paper we demonstrate how this model can be improved, by adding in a slow synaptic mechanism, leading first to a model with distributed delay. Moreover, we compare the past and present modelling approaches in terms of bifurcation structures, and show the existence of various transitions to SW dynamics.

The model we propose arises as a result of amalgamating a number of different theoretical viewpoints: a mean-field model to describe voltage responses in different brain regions, the corticothalamic loop and a wavelike equation to describe propagation of cortical activity. The history of the mean-field equations we use to model activity in each population may be traced back to the 1970s, where a number of seminal papers laid the foundations for relating theoretical studies to experimental and clinical data. For example, the works of Nunez [13] and Amari [14,15] were among the first to study brain activity from a spatially and temporally continuous viewpoint. The work of Amari may be in some sense considered a spatially extended version of the earlier work of Wilson and Cowan [16], who developed a temporally continuous firing rate model, whereas Nunez independently derived a spatiotemporal activity model; called the "brain-wave equation." Related to these mathematical descriptions of brain activity, Lopes da Silva [17] and Freeman [18], were amongst the first to describe phenomenologically, activity in large populations of neurons (neural masses), based upon the results of detailed experimental studies.

The second fundamental aspect of the model, is the incorporation of the corticothalamic loop. This loop has been implicated in a number of experimental and computational studies to be significant in the generation of sleep-spindles and generalized seizure activity [11,19,20]. From these studies, four main neuron types have been implicated in the generation of absence seizure activity. These are excitatory pyramidal cells and inhibitory interneurons in the cortex, and inhibitory reticular neurons and excitatory specific thalamic neurons in the thalamus.

The final important aspect of the model we consider, is the use of a wavelike equation to describe the propagation of cortical activity. A general formulation of this equation can be traced back to the work of Nunez [13,21], written in integral-differential form for an arbitrary choice of kernel used to describe spatial connectivity within the neural tissue. In the model we present, a specific choice of this kernel is made, described in Ref. [22], which enables us to write down a partial differential equation (PDE) description of the cortical propagation.

A final assumption we make is that the activity arising during absence seizures may be considered generalized to any specific cortical region, enabling the reduction of a PDE
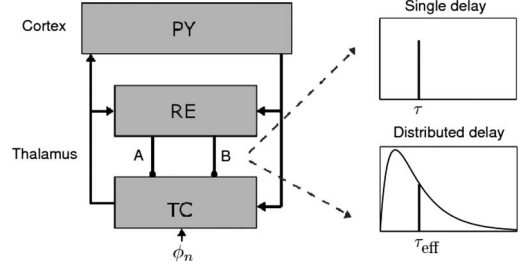

FIG. 2. Schematic of the thalamocortical model. Three neural populations (*e*, Re, Tc) are linked together via synaptic interactions. Arrows represent excitatory synaptic connections, dots represent inhibitory $GABA_A$ (label *A*) and $GABA_B$ (label *B*) receptors. A comparision is drawn between modeling $GABA_B$ with a single delay (as in our previous work [12]) or a distribution of delays $k(\tau)$ (as in the present study). We use the average of $k(\tau)$, τ_{eff} as a bifurcation parameter, to enable a comparison to be made.

description to an ODE model, where only spatially uniform solutions are considered. While this is a strong assumption, we believe that for the purposes of initial comparison with clinical EEG traces it is appropriate to seek a minimal model that could account for observed phenomena. Combining all of these results in the following corticothalamic model (depicted schematically in Fig 2):

$$\frac{d}{dt}\phi_e(t) = y(t),$$

$$\frac{d}{dt}y(t) = \gamma_e^2\{-\phi_e(t) + \mathsf{s}[V_e(t)]\} - 2\gamma_e y(t),$$

$$\frac{d}{dt}V_e(t) = z(t),$$

$$\frac{d}{dt}z(t) = \alpha\beta\{-V_e(t) + \nu_{ee}\phi_e(t) + \nu_{ei}\mathsf{s}[V_e(t)] + \nu_{eTc}\mathsf{s}[V_{Tc}(t)]\}$$
$$- (\alpha + \beta)z(t),$$

$$\frac{d}{dt}V_{Tc}(t) = w(t),$$

$$\frac{d}{dt}w(t) = \alpha\beta\{-V_{Tc}(t) + \nu_{Tcn}\phi_n + \nu_{Tce}\phi_e(t) + \nu_{TcRe}^A\mathsf{s}[V_{Re}(t)]$$
$$+ \nu_{TcRe}^B\phi_B(t)\} - (\alpha + \beta)w(t),$$

$$\frac{d}{dt}V_{Re}(t) = v(t),$$

$$\frac{d}{dt}v(t) = \alpha\beta\{-V_{Re}(t) + \nu_{Ree}\phi_e(t) + \nu_{ReTc}\mathsf{s}[v_{Tc}(t)]\}$$
$$- (\alpha + \beta)v(t). \tag{1}$$

Each of the neural masses (*e*=excitatory cortical neuron, Re=reticular nucleus, Tc=thalamocortical neurons) is de-

TABLE I. Parameter values for our model.

Quantity	Description	Values
$Q^{\max}$	Mean maximum firing rate of neural mass	$250 \ \text{s}^{-1}$
θ	Threshold of membrane potential before neural mass fires	$0.015 \ \text{V}$
σ	Standard deviation of neural mass firing	$0.006 \ \text{V}$
γ_e	Average ratio between pulse velocity and axon range	$100 \ \text{s}^{-1}$
α	Mean voltage response inverse decay time	$55 \ \text{s}^{-1}$
β	Mean voltage response inverse rise time	$220 \ \text{s}^{-1}$
ν_{ee}	Excitatory corticocortical coupling strength	$10 \times 10^{-4} \ \text{V s}$
ν_{ei}	Inhibitory corticocortical coupling strength	$-18 \times 10^{-4} \ \text{V s}$
$\nu_{e\text{Tc}}$	Thalamocortical to cortex coupling strength	$17 \times 10^{-4} \ \text{V s}$
$\nu_{\text{Tc}e}$	Cortex to thalamocortical coupling strength	is varied
$\nu_{\text{Tc}n}$	Subthalamic input strength	$40 \times 10^{-4} \ \text{V s}$
ν_{TcRe}^A	Reticular to thalamocortical strength (GABA$_A$)	$-8 \times 10^{-4} \ \text{V s}$
ν_{TcRe}^B	Reticular to thalamocortical strength (GABA$_B$)	$-8 \times 10^{-4} \ \text{V s}$
$\nu_{\text{Re}e}$	Cortex to reticular coupling strength	$0.5 \times 10^{-4} \ \text{V s}$
ν_{ReTc}	Thalamocortical to reticular coupling strength	$5 \times 10^{-4} \ \text{V s}$
a	GABA$_B$ inverse decay time	is varied
b	GABA$_B$ inverse rise time	is varied

scribed by its average membrane potential $V_a(t)$, where $a = e$, Re, Tc, and a sigmoidal function $\varsigma(\cdots)$ describing the average firing rate (see Table I). In addition, cortical excitatory neurons are described by a field variable $\phi_e(t)$ to take into account long-range cortico-cortical connections. In this investigation, we shall only consider spatially uniform solutions, leaving more general solutions as a next step in our research. The parameters ν_{ab} represent the weighting of inputs via synapses from population b onto population a. A more detailed description of these equations and the function $\varsigma(\cdots)$ appears in Ref. [12].

Inhibition of Tc cells by Re neurons in the thalamus has been found to be a crucial component in the development of SW activity [19] and thus we focus our attention on modeling two important receptors GABA$_A$ and GABA$_B$, which mediate this inhibition. In our previous work [12], we incorporated a time-delayed connection $\nu_{\text{TcRe}}^B \varsigma[V_{\text{Re}}(t-\tau)]$ with a fixed delay τ from Re to Tc populations. This served as a straightforward mechanism to account for a difference in time scales between GABA$_A$ and GABA$_B$; the inhibitory post-synaptic potential (IPSP) mediated by GABA$_B$ receptors has a much slower time scale than those mediated by GABA$_A$.

To account more appropriately for this discrepancy in time scales we introduce a firing rate $\phi_B(t)$, a slow variable governing the IPSPs of GABA$_B$. We obtain this by convolving the output firing rate of the Re population with a distributed delay kernel to account for the slow mediation of GABA$_B$ receptors

$$\phi_B(t) = \int_0^\infty k(\tau)\varsigma[V_{\text{Re}}(t-\tau)]d\tau, \qquad (2)$$

where the normalized kernel function $k(t)$ is given by

$$k(t) \equiv k(t;a_1,a_2) = \frac{a_1 a_2 (e^{-a_1 t} - e^{-a_2 t})}{a_2 - a_1}, \quad a_2 > a_1, \quad (3)$$

with a_1 and a_2 corresponding to rise and decay times, respectively. Our choice is motivated by existing modeling approaches, which put emphasis on physiological GABA$_B$ models (see [20] for single cell GABA$_B$ models, and Refs. [5,23] for neural population dynamics). These various models (linear and nonlinear) have one thing in common: if a sufficiently strong presynaptic input is given to activate GABA$_B$, the receptor responds with a current profile consisting of a steep rise and a slow decay (see Fig. 5.9 of Ref. [20] for an illustration). The double exponential function $k(t)$ is chosen because it mimics this particular behavior. Note that to keep our model simple, we do not use this approach to describe any other synapses (GABA$_A$, excitatory), we consider these faster timescales to be captured in the rise and decay time parameters (α, β) in Eq. (1).

An interesting comparison can be made with our previous work [12], where we effectively used $\phi_B(t) = \varsigma[V_{\text{Re}}(t-\tau)]$. Our present approach turns the corticothalamic model (1) into a distributed DDE. However, substituting the double exponential (3) as the kernel $k(t)$, enables us to employ the so-called "linear chain trick" [24] [essentially noting that $\phi_B(t)$ then satisfies a second order ODE] to reformulate our model (1)–(3) as a set of ten ODEs, as opposed to the set of eight DDEs in our previous investigations. It should be noted that the particular choice of $k(t)$ to mimic the rise and decay profile is not unique (see Ref. [25] for details).

It should be noted that in formulating the above equations, a number of assumptions have been made. By only considering spatially uniform solutions, long-range cortical-cortical connections are automatically neglected. In addition, we have not considered directly the activity of cortical interneu-
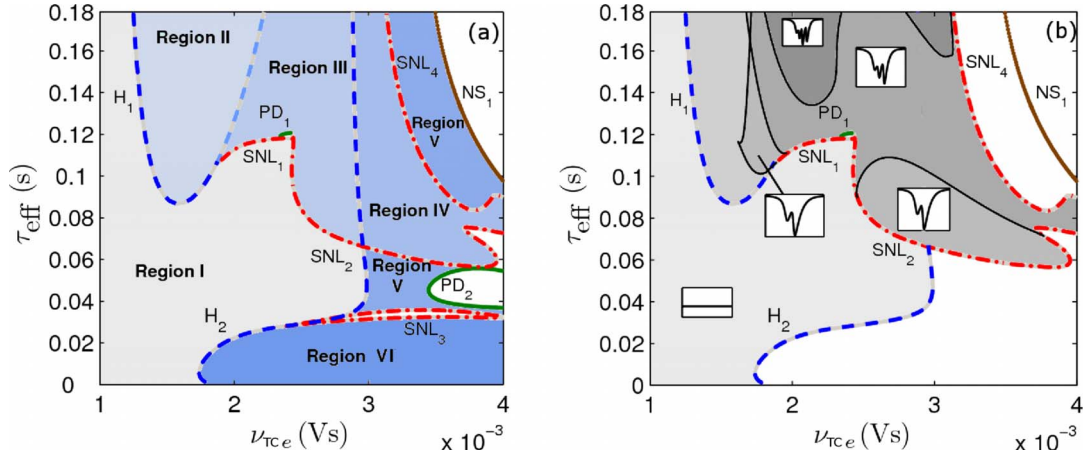
FIG. 3. (Color online) Two parameter analysis of our present model in the (ν_{Tce}, τ_{eff}) plane. (a) Curves of bifurcations (H=Hopf, SNL=saddle node of limit cycles, PD=period doubling, and NS=Neimark-Sacker) divide the plane into various dynamical regions. (I) contains only a steady state, (II) contains 2–3 Hz SW oscillations, (III) contains both steady state and SW oscillations, (IV) contains both SW oscillations and a fast 20 Hz oscillation, (V) contains only the 20 Hz oscillation, (VI) contains an α-like 11 Hz oscillation. White regions contain more complex dynamics, and are beyond the scope of the present paper. (b) We focus on all regions where our model supports 2–3 Hz oscillations (II, III, IV). In these regions we track the onset of spikes (black lines), using a spike-detection method explained in Ref. [9].

rons. A number of previous studies have reformulated the activity of this population in terms of a contribution from a negatively weighted pyramidal population (for example, Refs. [2,4]). The justifications given therein for this have included the synchronous firings of inhibitory and excitatory neural populations, as well as the relatively small numbers of interneurons and their possible contribution to EEG dynamics. While we do not justify this reduction on either of these grounds per se, having noted the qualitative agreement between model output and clinical EEG recordings, we feel it is appropriate to pursue this reduction as we wish to consider a minimal model whose well-defined mechanisms are sufficient to explain the origin of spike and wave discharges generated in the corticothalamic network. In the conclusion we discuss in more detail the possible consequences of the modeling assumptions we have made.

III. RESULTS

We perform a numerical bifurcation analysis of the system (1)–(3), using the continuation package MATCONT [26] and then compare these results with our past investigations with DDE-BIFTOOL, presented in Ref. [12,27]. To aid this comparison, we introduce a term relating the effective delay

$$\tau_{eff} = \int_0^\infty \tau k(\tau) d\tau = \frac{a_1 + a_2}{a_1 a_2}. \tag{4}$$

Our motivation for this choice is our past work with DDE-BIFTOOL, where we used the single GABA$_B$ delay as one of the key parameters in continuation. Because our new model has a delay distribution $k(t)$, we use this average time scale τ_{eff} (see Fig. 2) as a bifurcation parameter. To simplify our work, we will assume a fixed ratio $a_2/a_1 = 3$ (based on existing literature [23]), which ensures a one to one correspondence between a_1 and τ_{eff}. Further, the coupling ν_{Tce} from

cortical excitatory neurons (e) to thalamic Tc neurons has been used in past research [6,7,9,12] to study the onset of SW activity, and we employ it as a second bifurcation parameter in our present study.

The results of our bifurcation analysis in the two-dimensional (ν_{Tce}, τ_{eff}) plane are shown in Fig. 3(a). Branches of bifurcations divide the plane into various dynamical regions, of which (III, IV) are bistable. We find that if the average delay τ_{eff} is made large enough (80–100 ms, a characteristic time scale for GABA$_B$) our model supports 2–3 Hz SW activity. Interestingly, if $\tau_{eff} < 40$ ms the model supports 11 Hz α-like activity (region VI). Decreasing τ_{eff} to this order of magnitude can be viewed as introducing a mismatch between GABAergic receptors. Also, Fig. 3(b) displays the result of applying a spike-detection method [9] to track the onset of (poly)spikes in the 2–3 Hz solutions of our model. This clearly maps out how the specific shape of the 2–3 Hz solutions (wave, spike-wave, polyspike wave) depends on the model parameters.

In Fig. 4 we present a comparison between our present model and previous model with single delay [12]. Here panel (a) is an expanded version of the upper quadrant of Fig. 3(b). The bifurcation analysis performed on our previous model is shown in Fig. 4(b). In addition, some demonstrative time series are displayed. From Fig. 4 we find that in both models, the parameter ν_{Tce} can be used to make a transition from a steady state region to a SW oscillation [for example, fix $\tau_{eff} = 0.12$ s in Fig. 4(a) and increase ν_{Tce}]. An increase of (effective) delay leads to an increase of spikes in both models. Moreover, when the (effective) delay is decreased below a certain point, no SW oscillations are generated in either case. Note, however, that in Fig. 4(b), it is still possible to have ~3 Hz oscillations without spikes for $\tau \lesssim 40$ ms, whereas in our present model, we find instead 11 Hz activity (resembling α), which is in some sense more in keeping with clinical data.
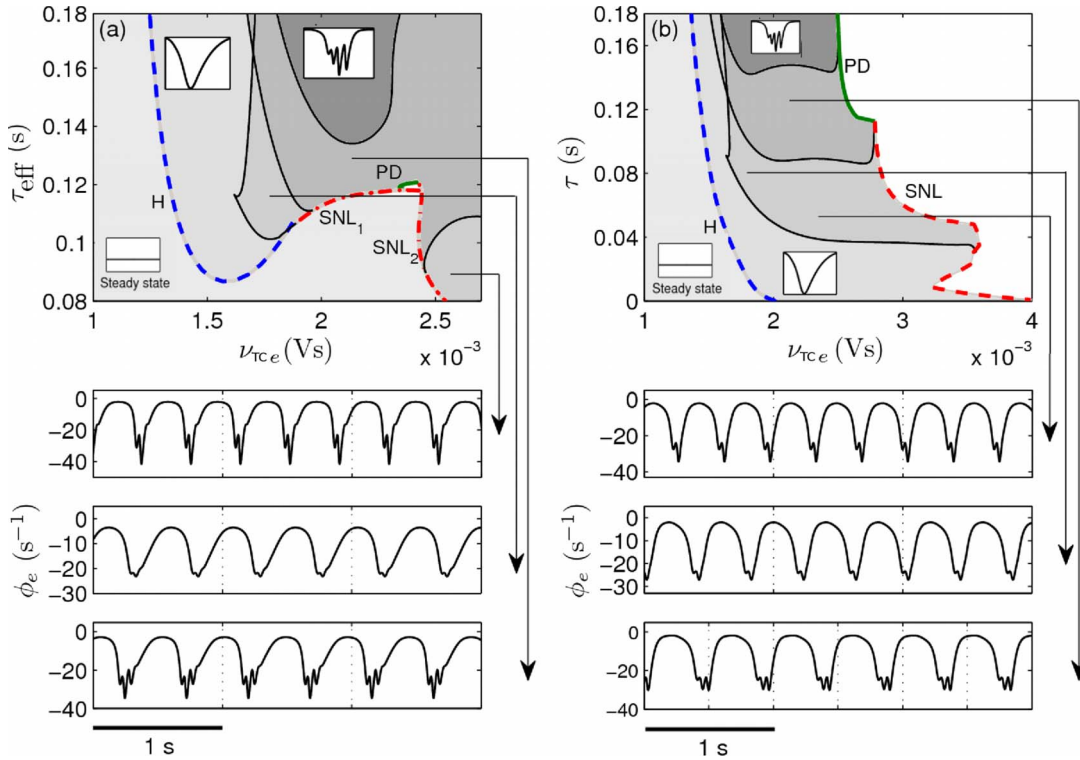
FIG. 4. (Color online) Comparing transitions between different spike and wave morphologies in the present ODE model (a) and our previous DDE model (b) [12]. Black solid curves in the top two panels indicate the points where an additional spike is added to $2-3$ Hz periodic solutions (see Fig. 1). In both models (a) and (b), SW oscillations only exist above a certain value of the (effective) delay.

In terms of modeling the onset of SW activity, our present model captures two fundamentally different mechanisms. First, a bifurcation from a preseizure state [such as region I in Fig. 3(a)] into SW activity by changing a parameter. Secondly a noise-induced transition from an interictal state to an SW attractor, in a bistable region of our model [for example, region III in Fig. 3(a)]. In Fig. 5 we show examples of these two transitions; in panels (a1), (a2) we simulate an episode of SW activity, by slowly ramping $\nu_{\mathrm{Tc}e}$. Alternatively, in panel (b) we keep all model parameters fixed in a bistable region, and observe transitions arising due to the subthalamic noise term [ϕ_n, see Eq. (1)]. This leads to episodes of SW activity, the precise statistics of which may be controlled by the levels of noise used. These mechanisms offer possible explanations for the graded/abrupt onsets observed in panels (c) and (d) of Fig. 1. Recall that some seizures gradually build up a ~ 3 Hz oscillation and develop a spike as time progresses, whereas others begin abruptly with spikes occurring in the first cycle. It is an important feature of the present model that both of these scenarios can be explained and makes it worthy of further consideration.

It should be noted that small regions of bistability were also observed in our original DDE model [12]. However, the region of bistable activity corresponded only to oscillatory activity (without spikes) and a steady state, meaning that this model could not explain an abrupt transition to spike and wave activity in the same manner (see Fig. 6).

IV. CONCLUSION

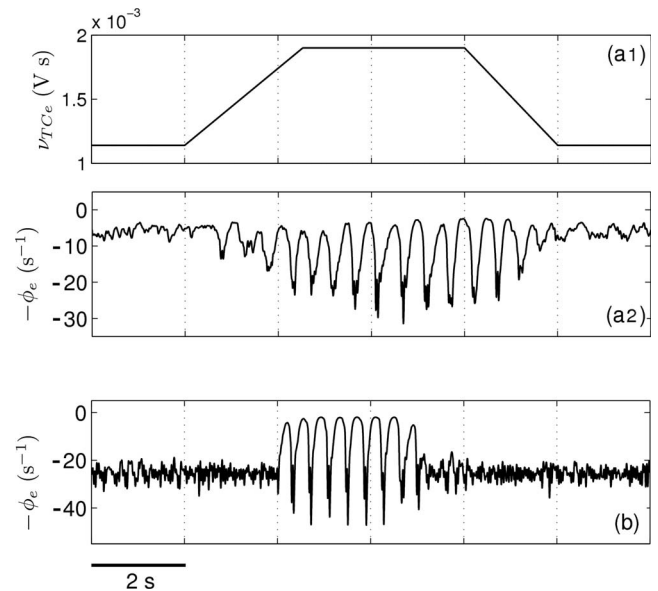In conclusion, we have shown how a neural-mass model can be enhanced by introducing an additional slow synaptic

FIG. 5. Illustrating the two mechanisms for the onset of SW activity. In panels (a1), (a2) the activity arises by varying a bifurcation parameter ($\nu_{\mathrm{Tc}e}$). In panel (b) bistability obtained by keeping parameters fixed and injecting subthalamic noise causes a transition to a seizurelike state. Note that in the second case, the spike is already present at the onset of oscillation. This can be compared to human EEG data (see Fig. 1) where some SW patterns measured during absence seizures start abruptly, whereas others grow from a sinusoidal-like oscillation over the initial cycles of the seizure.
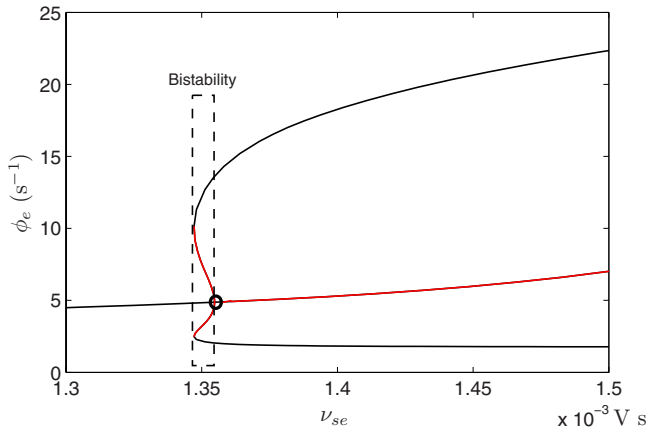
FIG. 6. (Color online) In the original DDE formulation of Ref. [12], a small region of bistability is observed, as the Hopf bifurcation in this model is subcritical for certain values of the delay τ. It should be noted in this case, that the first spike in this system does not occur for values of $\nu_{se} < 2.0 \times 10^{-3}$. Hence there is no bistability between a seizure state and an interictal state, only an oscillation and a steady state. Our new formulation which permits bistability between a seizure state and a steady state provides better agreement with observed clinical recordings [see panel (d) of Fig. 1, where spikes appear abruptly at seizure onset.

term to account for IPSPs due to slow $GABA_B$ inhibition in the thalamus. We used the linear chain trick to transform our system from one with a distributed delay to a system of ODEs. By considering the bifurcation structure of this model, we have studied how a variety of different types of dynamics, commonly observed in clinical EEG recordings of subjects with absence seizures, can arise. We find that our model permits different types of EEG dynamics over a wider regions of parameter space than was the case for the system of DDEs studies in Ref. [12]. In particular, the model permits a region of bistability between a spike and wave attractor and a steady-state corresponding to interictal-like dynamics. This scenario fits in with clinical recordings [see panel (d) of Fig. 1] that demonstrate an abrupt transition to seizure dynamics, with a prominent spike at seizure onset. Additionally graded onsets are also possible [panel (c) of Fig. 1] which are more akin to the bifurcation route through spike and wave activity, as a suitable parameter is varied.

It should be noted that we made a number of specific assumptions that permitted a reduction of the model equations from a PDE with delay, to an ODE without delay. These assumptions resulted in a number of physiological properties being discarded. For example, our model does not include direct intracortical inhibition, rather an assumption of synchronous firings of pyramidal cells and interneurons enables synaptic interactions of interneurons [ν_{ei} in Eq. (1)] to be a negatively weighted response of the firing rate of the pyramidal population (see, for example, Ref. [4]). While this assumption is difficult to justify physiologically, comparison

to clinical EEG recordings (as presented) make it reasonable in the current setting of developing a reduced model capable of capturing a wide variety of EEG dynamics. It will be desirable in future work to compare the output of the present model with a model which directly includes a population of inhibitory interneurons. We might speculate that adding such a population could create additional limit cycles in the system, due to the interaction between pyramidal cells and inhibitory cells. This raises the possibility of purely cortical spike and wave activity, as has been observed in athalamic cats [28] and studied in computational models [29]. We should point out that such activity is not believed to play a role in the types of typical absence seizures in humans that we consider in this work. The inclusion of populations of inhibitory interneurons in a purely cortical model has been considered in Ref. [3] and the relationship to some nonseizure EEG activity, for example, the α rhythm, was explored. A model of this type has also been considered to study the effects of anaesthesia on human EEG [31].

There are a number of advantages to considering an ODE formulation of a neural-mass model relative to the previously considered DDE description. For example, the level of system complexity is greatly reduced. In a DDE framework, even with a single fixed delay, the phase space of system becomes infinite, making rigorous analysis difficult. A further important application of this research is the linking of model predictions to clinical data. One way that this could be achieved would be the fitting of model parameters from the data. In the case of DDEs, robust techniques do not exist and only "brute force" methods based on large numbers of simulations may be used for estimation in this case. On the other hand, a number of robust methods have been developed for the fitting of parameters of ODE models. One such method, Potter's wheel) [30], provides a user-friendly interface for obtaining estimates of parameters, as well as estimates of goodness of fit. Our work in this area will be extended to explore the possibility of model predictions being used to develop schemes for the early detection and prediction of seizures. For example, it may be possible to track changes in model parameters estimated from clinical data in this manner described above and use these as a warning. Such an approach provides an exciting alternative approach to existing methods of seizure prediction based purely on data analysis techniques [32].

[1] B. J. Fisch, *Spehlmann's EEG Primer: Basic Principles of Digital and Analog EEG* 3rd ed. (Elsevier, Amsterdam, 2007).

[2] P. A. Robinson, C. J. Rennie, and J. J. Wright, Phys. Rev. E **56**, 826 (1997).

[3] D. T. J. Liley, P. J. Cadusch, and M. P. Dafilis, Network Comput. Neural Syst. **13**, 67 (2002).

[4] P. A. Robinson, C. J. Rennie, and D. L. Rowe, Phys. Rev. E **65**, 041924 (2002).

[5] P. Suffczynski, F. H. Lopes da Silva, J. Parra, D. Velis, and S. J. Kalitzin, Clin. Neurophysiol. **22**, 288 (2005).

[6] M. Breakspear, J. A. Roberts, J. R. Terry, S. Rodrigues, N. Mahant, and P. A. Robinson, Cereb. Cortex **16**, 1296 (2006).

[7] S. Rodrigues, J. R. Terry, and M. Breakspear, Phys. Lett. A **355**, 352 (2006).

[8] V. Shusterman and W. C. Troy, Phys. Rev. E **77**, 061911 (2008).

[9] S. Rodrigues, D. Barton, R. Szalai, O. Benjamin, M. P. Richardson, and J. R. Terry (unpublished).

[10] V. Crunelli and N. Leresche, Nat. Rev. Neurosci. **3**, 371 (2002).

[11] M. Steriade, *Neuronal Substrates of Sleep and Epilepsy* (Cambridge University Press, Cambridge, 2003).

[12] F. Marten, S. Rodrigues, O. Benjamin, M. P. Richardson, and J. R. Terry (unpublished).

[13] P. L. Nunez, Math. Biosci. **21**, 279 (1974).

[14] S. Amari, Biol. Cybern. **17**, 211 (1975).

[15] S. Amari, Biol. Cybern. **27**, 77 (1977).

[16] H. R. Wilson and J. D. Cowan, Biophys. J. **12**, 1 (1972).

[17] F. H. Lopes da Silva, A. Hoeks, H. Smits, and L. H. Zetterberg, Kybernetik **15**, 27 (1974).

[18] W. J. Freeman, *Mass Action in the Nervous System* (Academic Press, New York, 1975).

[19] A. J. Destexhe, J. Neurosci. **18**, 9099 (1998).

[20] A. Destexhe and T. J. Sejnowski, *Thalamocortical Assemblies* (Oxford University Press, Oxford, 2001).

[21] P. L. Nunez and R. Srinivasan, *Electric Fields of the Brain: The Neurophysics of EEG* (Oxford University Press, Oxford, 2006).

[22] V. K. Jirsa and H. Haken, Phys. Rev. Lett. **77**, 960 (1996).

[23] D. Golomb, E. Ahissar, and D. J. Kleinfeld, Neurophysiology **95**, 1735 (2006).

[24] J. M. Cushing, *Integrodifferential Equations and Delay Models in Population Dynamics, Lecture Notes in Biomathematics* (Springer Verlag, Berlin, 1977).

[25] P. C. Bressloff and S. Coombes, Neural Comput. **12**, 91 (2000).

[26] A. Dhooge, W. Govaerts, and Yu. A. Kuznetsov, ACM Trans. Math. Softw. **29**, 141 (2003).

[27] S. Rodrigues, D. A. W. Barton, F. Marten, M. Kibuuka, G. Alarcon, M. P. Richardson, and J. R. Terry (unpublished).

[28] M. Steriade and D. Contreras, J. Neurophysiol. **80**, 1439 (1998).

[29] A. Destexhe, D. Contreras, and M. Steriade, Neurocomputing **38**, 555 (2001).

[30] T. Maiwald and J. Timmer, Bioinformatics **24**, 2037 (2008).

[31] I. Bojak and D. T. J. Liley, Phys. Rev. E **71**, 041902 (2005).

[32] F. Mormann, R. G. Andrzejak, C. E. Elger, and K. Lehnertz, Brain **130**, 314 (2007).